Observation of whispering gallery modes from hexagonal ZnO microdisks using cathodoluminescence spectroscopy

Sumin Choi, Cuong Ton-That, Matthew R. Phillips, and Igor Aharonovich

Citation: Applied Physics Letters **103**, 171102 (2013); doi: 10.1063/1.4826481
View online: http://dx.doi.org/10.1063/1.4826481
View Table of Contents: http://scitation.aip.org/content/aip/journal/apl/103/17?ver=pdfcov
Published by the AIP Publishing

Observation of whispering gallery modes from hexagonal ZnO microdisks using cathodoluminescence spectroscopy

Sumin Choi, Cuong Ton-That, Matthew R. Phillips, and Igor Aharonovich[a)]
School of Physics and Advanced Materials, University of Technology Sydney, Ultimo, New South Wales 2007, Australia

(Received 8 September 2013; accepted 4 October 2013; published online 21 October 2013)

Zinc oxide hexagonal microdisks with diameters ranging from 3 μm up to 15 μm were fabricated by thermal chemical vapour deposition. Optical characterisation of ZnO microdisks was performed using low temperature (80 K) cathodoluminescence (CL) imaging and spectroscopy. The microdisks exhibited green luminescence locally distributed near the hexagonal boundary of the ZnO microdisks. High resolution CL spectra of the ZnO microdisks revealed whispering gallery modes (WGMs) emission. The experimentally observed WGMs were in excellent agreement with the predicted theoretical positions calculated using a plane wave model. This work could provide the means for ZnO microdisk devices operating in the green spectral range. [http://dx.doi.org/10.1063/1.4826481]

Wide band gap semiconductor optical resonators are of great importance in developing paradigms for optoelectronics and light emitting devices (LEDs). Zinc oxide (ZnO) is a promising wide band gap (~3.4 eV) semiconductor for the development of optical devices in the visible spectral range because of its highly efficient optical emission. ZnO is presently used in a variety of optoelectronic applications, such as LEDs, transparent semiconductors, piezoelectrics, and sensors.[1–4] In addition, the flexible control over ZnO growth enables bottom up engineering of ZnO micro- and nano-structures with various geometrical shapes and sizes (e.g., tetrapods, tapered nanowires, and mushrooms).[5–7] In particular, there is currently great interest in the bottom up fabrication of ZnO optical resonators that can confine and guide light for applications in photonics and quantum information processing.

Among other optical resonators, ZnO microdisks are of a particular interest. Microdisk resonators support propagation of whispering gallery modes (WGMs), enabling technologies such as bright LEDs, sensing, and low threshold lasers.[8–11] For the WGMs emission, the light wave propagates circularly around the interface of material/air due to multiple total internal reflections. As a result, the optical losses can be significantly reduced so that the WGMs can provide an attractive means to increase luminescence efficiency in optical resonators. However, fabrication of microdisks is non-trivial, as they require undercutting the active layer to achieve vertical light confinement.

Recently, numerous works on ZnO micro- and nanostructures with a moderate level of light confinement and increased luminescence efficiency were reported.[12–17] While some attributed the emission enhancement to the presence of WGMs, most of previous works showed excitonic WGM is in the ultraviolet range,[15,18–20] which is not suitable for visible applications. In addition, the ZnO structures were not well separated from each other, which make it challenging for realistic applications to WGMs resonators.

In this work, we demonstrate bottom up growth of well isolated ZnO microdisks on silicon dioxide substrate. Raman spectroscopy confirms the high quality of the ZnO material. High resolution cathodoluminescence (CL) studies clearly reveal that the resonators exhibit green emission and clear presence of WGMs with quality factors of ~60 and ~90 in ZnO microdisks of diameter 5 μm and 9 μm, respectively. The position of the WGMs is supported using a plane wave model.

To synthesize the ZnO microdisks, ZnO powder (200 mg) was mixed with graphite powder (200 mg) with a weight ratio of 1:1 and put into a small boat as a source material. The ZnO microdisks were grown on 1 μm thick thermally grown silicon dioxide on silicon in a horizontal tube furnace under ambient atmosphere. Catalysts and carrier gases were not used. Zn vapour was produced through the carbothermal reduction of ZnO powder by graphite, which acts as a reducing agent. The Zn vapour was then reoxidised by oxygen in air to facilitate the formation of ZnO microdisks. After heating the source material at 1050 °C for 5 min with the substrate at the same temperature, the source was immediately removed to limit the vertical growth to less than 10 μm. A large number of ZnO microdisks were formed on the substrate.

Figures 1(a) and 1(b) show scanning electron microscope (SEM) (Zeiss Supra 55VP) secondary electron images at 20 kV of the as-grown 5 μm diameter ZnO microdisk. The density of the microdisks changed across the substrate surface (not shown), but isolated ZnO microdisks were always observed due to the lack of nucleation sites and source materials, resulting in the ZnO forming sparsely. Controlled growth of isolated microdisks is vital for future devices fabrication and proper spectroscopy studies. The well-defined hexagonal symmetry of the top edge facets can be clearly seen from the microdisk in Figure 1(a). The diameters of the microdisks were in the range of 3 μm to 15 μm. Figure 1(b) shows side view of SEM image of an individual ZnO microdisk. It can be seen that the top of the microdisk has smooth edge facets that are likely to support WGMs propagation.

[a)]Email: Igor.aharonovich@uts.edu.au

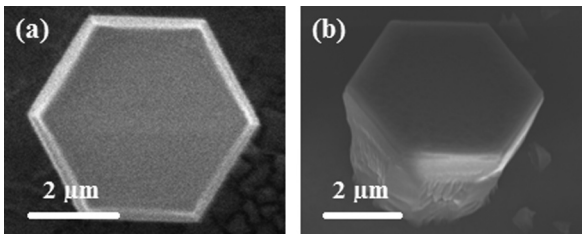

FIG. 1. (a) Top and (b) side-view SEM secondary electron images of ZnO microdisk at an operating voltage of 20 kV. A well-defined hexagonal shape is clearly visible.

Figure 2 shows the Raman spectrum recorded from the ZnO microdisk using 633 nm line of a Renishaw He-Ne laser. The peaks at 302 cm^{-1}, 520 cm^{-1}, and 618 cm^{-1} are associated with the silicon substrate. The intense Raman peak at 437 cm^{-1} is a typical Raman active branch of bulk wurtzite ZnO associated with the optical phonon E_2^{high} mode. In addition, other two peaks for the ZnO microdisk at 333 cm^{-1} and 379 cm^{-1} are visible and assigned to the E_2^{high} - E_2^{low} (multi-phonon process) and A_1 (longitudinal optical phonon) modes, respectively.[21] The full width half maximum (FWHM) of the E_2^{high} mode at 437 cm^{-1} is ~7 cm^{-1}, narrower than the typical reported values for ZnO structures (~12 cm^{-1}).[22] Thus, the narrow and strong E_2^{high} mode combined with a very weak A_1 mode confirm that the fabricated ZnO microdisks have predominantly wurtzite crystal structure.

To characterise the optical properties of the ZnO microdisks, CL measurement of the samples is carried out at 80 K with an accelerating voltage of 15 kV inside a SEM (FEI Quanta). The monochromatic CL image of the vertically grown and isolated hexagonal ZnO microdisk at 530 nm is shown in Figure 3(a). As can be seen in the image, the green luminescence is not distributed uniformly across the microdisk, but is locally concentrated at the hexagonal boundary of the microdisk. Figure 3(b) shows a CL spectrum of the side and centre regions, respectively. The beam positions are

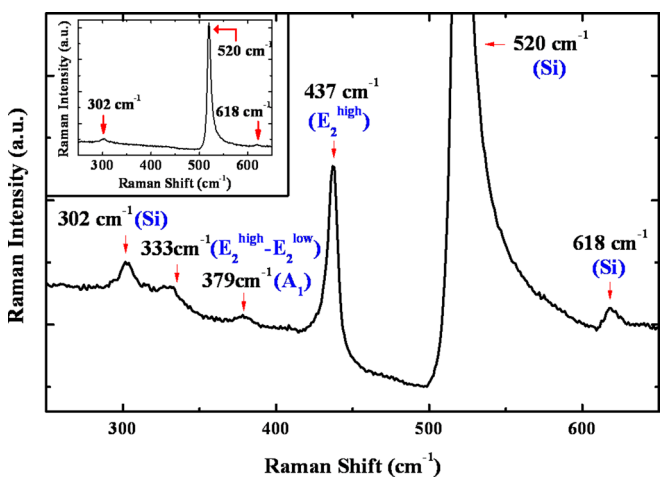

FIG. 2. Raman spectrum of the ZnO microdisk confirming a high quality wurtzite structure. The Raman peak at 437 cm^{-1} is associated with the hexagonal wurtzite ZnO optical phonon E_2^{high} mode. The strong peak at 520 cm^1 is associated with the silicon substrate. Inset is the Raman spectrum of a bare silicon substrate.

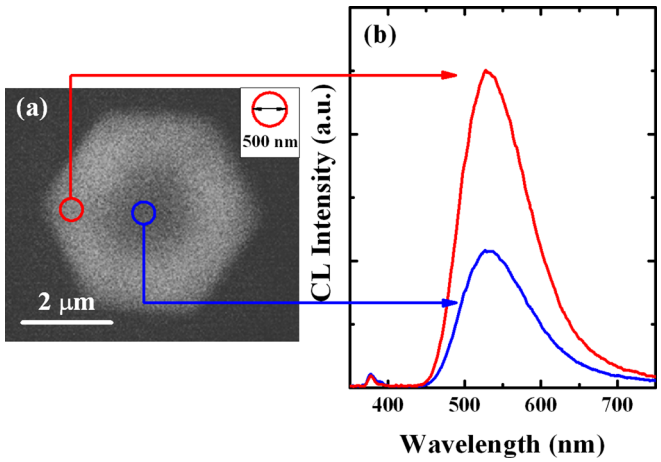

FIG. 3. (a) Monochromatic CL image of the ZnO microdisk at 530 nm at 15 kV. (b) Representative CL spectra recorded from the side region and the centre region of the ZnO microdisk. The local excitation spots are indicated by red and blue circles in (a). Inset of Figure 3(a) is the lateral spread of the interaction volume of the electron beam at 15 kV. There is a significant difference of green emission between the side and the centre regions.

marked as red and blue circles. The excitonic emission peak at 378 nm is almost equal in intensity at the boundary and centre of the microdisk. The stronger peak at the green spectral range, centred at around 530 nm, is the green emission from the ZnO. The chemical origin of this green emission is still not well understood, even though green luminescence is attributed to intrinsic defects such as oxygen vacancies and zinc vacancies and complexes or extrinsic impurities, such as Cu.[23,24] As can be seen in Figure 3(b), the luminescence intensity of the green emission is significantly stronger near the boundary of the microdisk, likely to be enhanced by the total internal reflection of light within the microdisk. Such an enhancement is often associated with the presence of WGMs, as discussed below. CASINO Monte Carlo modeling of the electron interaction volume at 15 kV shows that the lateral spread of the electron beam in ZnO is <500 nm (represented by a circle in the inset of Figure 3(a)) indicating that the increase in green luminescence towards the periphery of the ZnO microdisk is not related to excitation artifacts due to forward scattered electrons.[25]

To investigate the green luminescence in more detail, high resolution CL spectra (0.05 nm/pixel, Hamamatsu CCD detector) from the periphery of the ZnO microdisks were recorded. The typical CL spectra of a 5 μm and a 9 μm microdisks are shown in Figures 4(a) and 4(b), respectively. Each CL spectrum clearly shows the evolution of the WGMs. As expected, the disk with larger diameter exhibits narrower spacing between the observed resonator modes. The size dependence of the structured green CL spacing confirms that the enhanced edge emission in the ZnO microdisks is clearly unrelated to increased surface emission widely reported in ZnO nanowires due to surface band bending effects or an increased concentration of surface defects.[26,27] The energy spacing between the emission peaks from the 5 μm and 9 μm microdisks is in the range of 23–24 meV and 34–40 meV, respectively. These spacing values are significantly smaller than the longitudinal optical (LO) phonon energy of 72 meV, indicating they are not related to the vibronic states as reported previously by Reynolds *et al.*[28]

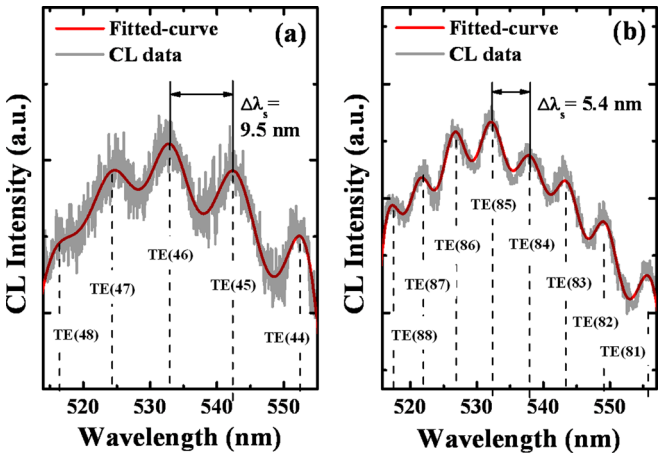

FIG. 4. (a), (b) High resolution CL spectra from the peripheral area of the ZnO microdisk shows a series of peaks corresponding to WGMs with a green emission band using Lorentzian deconvolution method. The integers are the mode numbers for respective resonant mode peaks: (a) 5 μm and (b) 9 μm of the microdisks.

The spectra were fitted to a sum of multi-peaks using the Lorentzian deconvolution method centred at each resonant wavelength as shown in Figures 4(a) and 4(b) (fitted red curve). Five and eight Lorentzian distributions reproduced the CL spectra reasonably well. The dashed lines in Figures 4(a) and 4(b) represent predicted 5 and 8 discrete optical mode numbers of WGMs located at each resonant peak for small and large microdisks.

For optical resonators, it is important to analyse the observed resonance to understand the nature of the light confinement. Below, we analyse the mode spacing and the mode resonances to show that the ZnO microdisks support the propagation of WGMs. We first analyse the mode spacing using a classical plane wave model. For possible resonant modes, the mode spacing $d\lambda_s$ is defined as

$$\Delta\lambda_s = \frac{\lambda^2}{L\left(n - \lambda\frac{dn}{d\lambda}\right)}, \tag{1}$$

where λ is the resonant wavelength, L is the cavity path length, n is the refractive index of ZnO, and the $dn/d\lambda$ is the Sellmeier's first-order dispersion relation. The wavelength-dependent refractive indices of the ZnO microdisk described by the Sellmeier's dispersion function were used to investigate which polarisation mode was formed in the microdisks for transverse electric (TE) and magnetic (TM) modes (see supplementary material for a refractive index simulation[29]). For all of the calculations, two different sizes of the ZnO microdisks were chosen (5 μm and 9 μm) to establish which modes were formed to the microdisks. For WGMs, the calculated spacing is 9.6 nm and 5.3 nm for small and large microdisks, respectively, which is in an excellent agreement with the experimentally observed mode spacing shown in Figure 4. If the modes were Fabry-Pérot modes, the calculated mode spacing at 533 nm would have been 14.4 nm and 8.0 nm, respectively, almost twice as larger than the experimental values.

We now analyse the spectral resonances of the observed modes. For hexagonal cavities, the constructive interference condition over multiple circulations is given by

$$\lambda_{WGM} = \frac{3\sqrt{3}nR}{N + \frac{6}{\pi}\arctan(\beta\sqrt{3n^2 - 4})}, \tag{2}$$

where N is the interference order, R is the side length of a hexagonal cavity, and n is the refractive index, $\beta = n^{-1}$ for TM or $\beta = n$ for TE polarisation.[15,30] Resonant wavelength of WGMs model with TE mode satisfies the experimentally observed peak positions with error <1 nm. The dashed lines in Figures 4(a) and 4(b) represent calculated 5 and 8 discrete optical mode numbers located at each resonant peak for small and large microdisks for WGMs for TE polarisation modes. The constructive interference at the green emission band is formed with the resonant wavelength of 533 nm when the integer N is 46 and 85 for small and large microdisks, respectively. Thus, the improved green CL intensity along its propagation path and its enhancement towards the edge of the hexagonal boundary of the ZnO microdisks is attributed to the WGMs enhanced emission. The WGMs observed from our ZnO microdisks were mostly TE polarised since typically TM polarised emission is much weaker and broader than TE modes.[14] The excellent agreement between the experimental results and the calculations of the mode spacing and the mode resonances confirms that the observed modes are WGMs that propagate laterally at the top surface of the microdisk.

The Q factor of the microdisk is given by $Q = \lambda / \Delta\lambda$, where λ and $\Delta\lambda$ are the peak wavelength and its FWHM, respectively. Therefore, the corresponding Q factors are $\sim$60 and 90 for smaller and larger microdisks, respectively. The relatively low Q factor is mostly due to the poor vertical confinement of light and contribution from losses such as defect absorption. Further improvement of the device is possible by limiting the vertical growth of the microdisk; therefore, creating a properly undercut structure.

In summary, ZnO microdisk resonators were grown vertically and sparsely on silicon dioxide substrates without catalysts, templates, and carrier gases. The Raman data show that the material is predominantly hexagonal ZnO. Monochromatic CL images and spectra of the ZnO microdisks showed that green luminescence is dramatically enhanced at the hexagonal boundary of the ZnO microdisks. High spectral resolution CL measurements revealed WGMs presence with moderate quality factors. Theoretical analysis of the wave propagation inside the resonator confirms that the observed resonances are WGMs. Further studies to realise ZnO resonators with higher quality factors by isolating the top layer through undercut will be of a great importance to improve the ZnO devices. Our results indicate that the ZnO microdisks may be a prime candidate for the advance of microdisk green LEDs and other applications in photonics and quantum information.

Dr. Aharonovich is the recipient of an Australian Research Council Discovery Early Career Research Award (Project Number DE130100592). Support from the Australian Research Council Grant DP0986951 was gratefully acknowledged. The authors would like to thank G. McCredie for technical support.

[1]R. Konenkamp, R. C. Word, and C. Schlegel, Appl. Phys. Lett. **85**, 6004–6006 (2004).
[2]A. Menzel, K. Subannajui, F. Guder, D. Moser, O. Paul, and M. Zacharias, Adv. Funct. Mater. **21**, 4342–4348 (2011).
[3]C. Pan, L. Dong, G. Zhu, S. Niu, R. Yu, Q. Yang, Y. Liu, and Z. L. Wang, Nat. Photonics **7**, 752–758 (2013).
[4]K. Nomura, H. Ohta, K. Ueda, T. Kamiya, M. Hirano, and H. Hosono, Science **300**, 1269–1272 (2003).
[5]Z. Zhang, H. Yuan, Y. Gao, J. Wang, D. Liu, J. Shen, L. Liu, W. Zhou, S. Xie, and X. Wang, Appl. Phys. Lett. **90**, 153116 (2007).
[6]P. Yang, H. Yan, S. Mao, R. Russo, J. Johnson, R. Saykally, N. Morris, J. Pham, R. He, and H.-J. Choi, Adv. Funct. Mater. **12**, 323 (2002).
[7]B. Wang, X. Jin, H. Wu, and Z. Zheng, J. Appl. Phys. **113**, 034313 (2013).
[8]S. Chang, N. B. Rex, R. K. Chang, G. Chong, and L. J. Guido, Appl. Phys. Lett. **75**, 166–168 (1999).
[9]X. Liu, W. Fang, Y. Huang, X. H. Wu, S. T. Ho, H. Cao, and R. P. H. Chang, Appl. Phys. Lett. **84**, 2488 (2004).
[10]H. Dong, Z. Chen, L. Sun, J. Lu, W. Xie, H. H. Tan, C. Jagadish, and X. Shen, Appl. Phys. Lett. **94**, 173115 (2009).
[11]K. Srinivasan, M. Borselli, and O. Painter, Opt. Express **14**, 1094–1105 (2006).
[12]J. Liu, Q. M. Ngo, K. H. Park, S. Kim, Y. H. Ahn, J.-Y. Park, K. H. Koh, and S. Lee, Appl. Phys. Lett. **95**, 221105 (2009).
[13]H. Yan, J. Johnson, M. Law, R. He, K. Knutsen, J. R. McKinney, J. Pham, R. Saykally, and P. Yang, Adv. Mater. **15**, 1907–1911 (2003).
[14]J. Dai, C. X. Xu, R. Ding, K. Zheng, Z. L. Shi, C. G. Lv, and Y. P. Cui, Appl. Phys. Lett. **95**, 191117 (2009).
[15]C. Kim, Y.-J. Kim, E.-S. Jang, G.-C. Yi, and H. H. Kim, Appl. Phys. Lett. **88**, 093104 (2006).
[16]D. J. Gargas, M. C. Moore, A. Ni, S. W. Chang, Z. Zhang, S. L. Chuang, and P. Yang, ACS Nano **4**, 3270–3276 (2010).
[17]D. Wang, H. W. Seo, C.-C. Tin, M. J. Bozack, J. R. Williams, M. Park, and Y. Tzeng, J. Appl. Phys. **99**, 093112 (2006).
[18]R. Chen, B. Ling, X. W. Sun, and H. D. Sun, Adv. Mater. **23**, 2199–2204 (2011).
[19]K. Okazaki, T. Shimogaki, K. Fusazaki, M. Higashihata, D. Nakamura, N. Koshizaki, and T. Okada, Appl. Phys. Lett. **101**, 211105 (2012).
[20]C. Czekalla, C. Sturm, R. Schmidt-Grund, B. Cao, M. Lorenz, and M. Grundmann, Appl. Phys. Lett. **92**, 241102 (2008).
[21]Y. Xing, Z. Xi, Z. Xue, X. Zhang, J. Song, R. Wang, J. Xu, Y. Song, S. Zhang, and D. Yu, Appl. Phys. Lett. **83**, 1689–1691 (2003).
[22]A.-J. Cheng, Y. Tzeng, H. Xu, S. Alur, Y. Wang, M. Park, T.-h. Wu, C. Shannon, D.-J. Kim, and D. Wang, J. Appl. Phys. **105**, 073104 (2009).
[23]K. Vanheusden, W. Warren, C. Seager, D. Tallant, J. Voigt, and B. Gnade, J. Appl. Phys. **79**, 7983–7990 (1996).
[24]C. Ton-That, L. Weston, and M. R. Phillips, Phys. Rev. B **86**, 115205 (2012).
[25]D. Drouin, A. R. Couture, D. Joly, X. Tastet, V. Aimez, and R. Gauvin, Scanning **29**, 92–101 (2007).
[26]W. Dake and R. Nicholas, ISRN Condens. Matter Phys. **2012**, 1–6.
[27]M. Foley, C. Ton-That, and M. R. Phillips, Appl. Phys. Lett. **93**, 243104 (2008).
[28]D. C. Reynolds, D. C. Look, and B. Jogai, J. Appl. Phys. **89**, 6189–6191 (2001).
[29]See supplementary material at http://dx.doi.org/10.1063/1.4826481 for a refractive index simulation.
[30]T. Nobis, E. M. Kaidashev, A. Rahm, M. Lorenz, and M. Grundmann, Phys. Rev. Lett. **93**, 103903 (2004).